

Stability Region of Hybrid Uplink NOMA: Game Theoretic Perspective

Jun-Bae Seo ¹, Bang Chul Jung ¹, *Senior Member, IEEE*,
Hu Jin ², *Senior Member, IEEE*,
and Jinho Choi ³, *Senior Member, IEEE*

Abstract—In this paper, we investigate stability region of hybrid uplink non-orthogonal multiple access (NOMA) in conjunction with non-cooperative game, where two users independently send packets with transmit power control according to fading channel gain to the same radio resource so that their packets are received at a base station (BS) with one of two target receive powers (TRPs). The BS then tries to decode the packets with successive interference cancellation (SIC) technique in power domain. We consider a symmetric non-cooperative game where the users (or players) send packets with one of two TRPs or no transmission. We examine the convexity of stability region at the mixed-strategy Nash equilibrium (NE) of the game, where no one's queue grows to infinity. Furthermore, we investigate how the stability region changes depending on the parameters of users' payoff.

Index Terms—Hybrid uplink NOMA, stability region, random access, truncated channel inversion, Nash equilibrium.

I. INTRODUCTION

Along with explosive research attention on downlink power-domain non-orthogonal multiple access (NOMA) [1], uplink NOMA has started to draw attention for the fifth generation (5G) new radio (NR). Two types of NOMA can be considered for uplink: code-domain [2], [3] and power-domain [4]–[13]. The former allocates a unique spreading code to each user, while the latter allows multiple users to send signals with superposition coding over the same time/frequency resource block. Additionally, the base station (BS) in power-domain NOMA tries to decode the superimposed signals from multiple users with successive interference cancellation (SIC) technique in a descending order of the received power. To facilitate SIC decoding at the BS, the users can control their transmit power such that the receive power of their packets at the BS can be one of the predefined levels, which is called target receive power (TRP) in [11]–[13]. The BS can try to decode the packet with the highest TRP.

As a distributed scheduling by random access, a hybrid uplink NOMA has been proposed in [13]. In the system, its bandwidth is

Manuscript received September 25, 2020; revised January 20, 2021; accepted March 10, 2021. Date of publication March 17, 2021; date of current version May 5, 2021. This work was supported in part by the National Research Foundation of Korea (NRF) through the Basic Science Research Program funded by the Ministry of Science and ICT (MSIT) under Grant NRF2019R1A2B5B01070697, in part by NRF Grant funded by the Korean Government (MSIT) under Grant NRF-2017K1A3A1A19071179, and in part by the Development Fund Foundation, Gyeongsang National University, 2020. The review of this article was coordinated by Dr. Vuk Marojevic. (*Corresponding authors: Hu Jin; Bang Chul Jung.*)

Jun-Bae Seo is with the Department of Information and Communication Engineering, Gyeongsang National University, Tongyeong 53064, South Korea (e-mail: jbseo@gnu.ac.kr).

Bang Chul Jung is with the Department of Electronics Engineering, Chungnam National University, Daejeon 34134, South Korea (e-mail: bcjung@cnu.ac.kr).

Hu Jin is with the Division of Electrical Engineering, Hanyang University, Ansan 15588, South Korea (e-mail: hjin@hanyang.ac.kr).

Jinho Choi is with the School of Information Technology, Deakin University, Geelong, VIC 3220, Australia (e-mail: jinho.choi@deakin.edu.au).

Digital Object Identifier 10.1109/TVT.2021.3066152

divided into M orthogonal radio resource blocks (RRBs). Each RRB is allocated to two users so that they can share it with uplink NOMA random access. Accordingly, the hybrid uplink NOMA supports a total of $2M$ users with M RRBs, while conventional orthogonal multiple access (OMA) can do M users. Since the hybrid uplink NOMA can achieve a statistical multiplexing based on random access, it is different from uplink NOMA random access [12], where a large number of users (re)transmit their (short) packet to an RRB at will.

As a prior work, using evolutionary game approach, it was shown in [13] how the users (or players) determine their strategy of choosing a TRP to maximize their payoff under the assumption that the users have always packets to send in their queues. However, the assumption on the saturated users may not be valid in practice.

In contrast, this paper investigates the stability region of the hybrid uplink NOMA system [13], by assuming that the users have a queue of unlimited length to store arriving packets. It can be said that any mean rate inside the stability region guarantees that the users' queue grows finite. In other words, if the mean rate of packet arrivals of any user lies outside the stability region, i.e., instability region, the user's queue grows infinite such that the packets in the queue experience infinite queuing delay.

The main contribution of this paper is to show how the stability region of hybrid uplink NOMA system can change when the users play a non-cooperative game of random access. More precisely, incorporating the game theory into the stability region enables the users to have incentive and/or disincentive of taking an action, which affects the shape of the stability region of their queues. Although the stability regions of some downlink and uplink NOMA systems have been investigated in [1] and [9], respectively, game theoretic perspective has not been incorporated with stability region. As a result, we show that the hybrid uplink NOMA system can achieve the stability region of the ideal time division multiple access (TDMA) system when the users have a high reward of transmission success and/or low transmission cost.

II. SYSTEM MODEL

A. Hybrid Uplink NOMA

Suppose a time-division duplex (TDD) system, whose time axis is divided into slots of a constant length. A slot is further divided into two parts, i.e., downlink and uplink. A BS serves a total of $2M$ users and assigns two users, say user 1 and 2, to one RRB for them to share in a slot [13]. We assume that the BS broadcasts a pilot signal over the downlink so that each user is able to estimate the channel gain, which is denoted by h_i for user $i \in \{1, 2\}$. We further assume block rayleigh fading channels, where h_i remains unchanged within a slot interval and varies randomly and independently slot by slot. Let $\gamma_i = |h_i|^2$ which is also known at user i . Owing to the channel reciprocity in TDD, user $i \in \{1, 2\}$ determines his transmit power $\mathcal{P}(\gamma_i)$ based on γ_i as follows:

$$\mathcal{P}(\gamma_i) = \begin{cases} \frac{P_k}{\gamma_i}, & \text{for } \tau_k \leq \gamma_i < \tau_{k-1} \\ 0, & \text{for } \gamma_i \leq \tau_2, \end{cases} \quad (1)$$

where P_k and τ_k for $k \in \{1, 2\}$ denote a TRP at the BS and $P_1 > P_2$ and a threshold for a user to determine TRP P_k . Additionally, we set $\tau_0 = \infty$.

Let us denote by $x_i = [p_i \ q_i \ r_i]$ the transmission probability vector of user i , where p_i and q_i denote the probability of γ_i being greater than τ_1 , and the probability of γ_i being in the interval between τ_1 and

τ_2 , respectively. We also have $r_i = 1 - p_i - q_i$. For Rayleigh fading channel, γ_i follows an exponential distribution. Assuming its mean by $\bar{\gamma}$, we can find τ_1 as

$$p_i = \Pr[\gamma_i \geq \tau_1] = e^{-\frac{\tau_1}{\bar{\gamma}}} \Rightarrow \tau_1 = \bar{\gamma} \ln \frac{1}{p_i}. \quad (2)$$

Furthermore, τ_2 can be found as

$$p_i + q_i = \Pr[\gamma_i \geq \tau_2] = e^{-\frac{\tau_2}{\bar{\gamma}}} \Rightarrow \tau_2 = \bar{\gamma} \ln \frac{1}{p_i + q_i}. \quad (3)$$

In the slot allocated to them, when user 1 chooses his TRP P_1 and user 2 chooses P_2 , the received signal at the BS is

$$\mathbf{z} = h_1 \sqrt{\frac{P_1}{\gamma_1}} \mathbf{s}_1 + h_2 \sqrt{\frac{P_2}{\gamma_2}} \mathbf{s}_2 + \mathbf{n}, \quad (4)$$

where \mathbf{s}_k represents the (coded) signal block of user k with $E[\mathbf{s}_k] = 0$ and $E[\mathbf{s}_k \mathbf{s}_k^H] = \mathbf{I}$, and $\mathbf{n} \sim \mathcal{CN}(0, N_0 \mathbf{I})$ is the background noise.

In NOMA, the strong signal in (4), i.e., signal with P_1 , is first decoded and then it is subtracted from \mathbf{z} . Then, the BS decodes user 2's signal. Both of users' transmissions can be successfully decoded, if P_1 and P_2 satisfy

$$\frac{P_1}{P_2 + N_0} \geq \theta \quad \text{and} \quad \frac{P_2}{N_0} \geq \theta, \quad (5)$$

where θ represents the signal-to-interference-plus-noise ratio (SINR) threshold for successful decoding. If the two users choose the same TRP, it results in unsuccessful SIC and no one can successfully transmit their signals.

Let us consider the queueing process of two users who share one RRB. We assume that each user has a queue of unlimited length to store incoming packets, whereas packets arrive at user i 's queue according to a Poisson process with mean rate λ_i (packets/slot) for $i \in \{1, 2\}$ just after each slot. We denote by A_i the packet arrivals of user i during one slot and by $Q_i(t)$ the queue length of user i at slot t . In the course of time, $Q_i(t)$ evolves as $Q_i(t) = \max\{0, Q_i(t-1) - B_i + A_i\}$, where B_i takes one if user i makes a successful transmission; otherwise, $B_i = 0$.

In order to incorporate game theory, let us consider a non-cooperative game for uplink NOMA random access: When each user makes a successful transmission, he gets reward R , which can be a function of $\log(1 + \theta)$ due to (5). On the other hand, the user with TRP $P_k \in \{1, 2\}$ should pay transmission cost C_k for $C_1 \geq C_2$. Then, the utilities that user 1 gets upon a successful transmission with TRP P_1 and P_2 are expressed as $u_1(1) = R(1 - p_2) - C_1$, and $u_1(2) = R(1 - q_2) - C_2$, respectively, whereas he gets $u_1(3) = 0$ when not transmitting. User 2 has also his utility $u_2(j)$ for $j \in \{1, 2, 3\}$, where p_2 and q_2 are replaced with p_1 and q_1 . Using the indifference principle, i.e., $u_1(1) = u_1(2) = u_1(3)$ and $u_2(1) = u_2(2) = u_2(3)$, the mixed-strategy Nash equilibrium (NE) denoted by p_i^* , q_i^* , and r_i^* for $i \in \{1, 2\}$ can be obtained as

$$p_i^* = 1 - \frac{C_1}{R} \quad q_i^* = 1 - \frac{C_2}{R}, \quad \text{and} \quad r_i^* = \frac{C_1 + C_2}{R} - 1, \quad (6)$$

where we have used $p_i^* + q_i^* + r_i^* = 1$. For p_i^* , q_i^* , $r_i^* \in [0, 1]$, we should have $R > C_1$, $C_1 + C_2 > R$, and $C_1 > C_2$.

Although it is shown in [13] how other mixed-strategy NEs depend on R , C_1 , and C_2 and how R , C_1 , and C_2 can be mapped to the thresholds τ_1 and τ_2 in (2), to make this work self-contained, we recapitulate how the mixed-strategy NE in (6) can be determined with τ_i in (2) and (3) as follows. Let us assume that C_i is a function of the average power consumption with TRP P_i , e.g., $C_i = c_i f(\bar{P}_i)$, where c_i is a scaling

factor and \bar{P}_i is the average power consumption with TRP P_i . Using (2) and (3), we can write C_1 and C_2 respectively as

$$\begin{aligned} C_1 &= c_1 \bar{P}_1 = c_1 P_1 \mathbb{E} \left[\frac{1}{\gamma_i} \mid \gamma_i \geq \tau_1 \right] = \frac{c_1 P_1}{p_i} \int_{\tau_1}^{\infty} \frac{1}{\gamma_i} \frac{1}{\bar{\gamma}} e^{-\frac{\gamma_i}{\bar{\gamma}}} d\gamma_i \\ &= \frac{c_1 P_1}{p_i \bar{\gamma}} E_1 \left(\frac{\tau_1}{\bar{\gamma}} \right) = \frac{c_1 P_1}{p_i \bar{\gamma}} E_1 \left(\ln \frac{1}{p_i} \right), \end{aligned} \quad (7)$$

where $E_1(x) = \int_x^{\infty} \frac{e^{-t}}{t} dt$, and

$$\begin{aligned} C_2 &= c_2 P_2 \mathbb{E} \left[\frac{1}{\gamma_i} \mid \tau_2 \leq \gamma_i \leq \tau_1 \right] \\ &= \frac{c_2 P_2}{q_i \bar{\gamma}} \int_{\tau_2}^{\tau_1} \frac{1}{x} e^{-x} dx = \frac{c_2 P_2}{q_i \bar{\gamma}} \left[E_1 \left(\frac{\tau_2}{\bar{\gamma}} \right) - E_1 \left(\frac{\tau_1}{\bar{\gamma}} \right) \right] \\ &= \frac{c_2 P_2}{q_i \bar{\gamma}} \left[E_1 \left(\ln \frac{1}{p_i + q_i} \right) - E_1 \left(\ln \frac{1}{p_i} \right) \right]. \end{aligned} \quad (8)$$

For the case of symmetric game, i.e., $p_1 = p_2$, and $q_1 = q_2$, using (6) and (7) we determine p_i^* as

$$R(1 - p_i^*) = \frac{c_1 P_1}{p_i^* \bar{\gamma}} E_1 \left(\ln \frac{1}{p_i^*} \right). \quad (9)$$

Once p_i^* is determined from the above, we can also determine q_i^* as

$$R(1 - q_i^*) = \frac{c_2 P_2}{q_i^* \bar{\gamma}} \left[E_1 \left(\ln \frac{1}{p_i^* + q_i^*} \right) - E_1 \left(\ln \frac{1}{p_i^*} \right) \right]. \quad (10)$$

Notice that the left-hand side (LHS) of (9) and (10) is a decreasing function of p_i^* or q_i^* in the unit interval, respectively. In [13], it is shown that the right-hand side (RHS) of (9) and (10) is an increasing function of p_i^* or q_i^* such that the uniqueness of p_i^* and q_i^* in (9) and (10) is guaranteed.

B. Stability Region and Stochastic Dominant Systems

Let us recall that 2 M users can be accommodated in hybrid uplink NOMA system with M RBBs. We only focus on a two-user queueing process since they share one RBB as mentioned earlier. The queueing process of two-user system is described as a two dimensional vector process $\mathbf{Q}(t) = [Q_1(t) \ Q_2(t)]$ for $t = 1, 2, \dots$. The system is said to be stable if we have

$$\lim_{t \rightarrow \infty} \Pr[\mathbf{Q}(t) < \mathbf{y}] \triangleq F(\mathbf{y}) \quad \text{and} \quad \lim_{\mathbf{y} \rightarrow \infty} F(\mathbf{y}) = 1. \quad (11)$$

Denote by $\Lambda_{\mathbf{x}} = [\lambda_1, \lambda_2]$ the stability region *conditioned* on the transmission probability vector $\mathbf{x} = [x_1 \ x_2]$, where (11) holds. In this paper, this is simply called stability region.

Let us now introduce the stochastic dominant systems. To begin with, we denote by \mathcal{S} a two-user system, which is called the *original* system. Besides system \mathcal{S} , we also consider its stochastic dominant system, where one or more users are designated (stochastic) *dominant* user who can have dummy packets upon their empty queue and transmit either a dummy or real packet at the head of queue. For a two-user system, we have three stochastic dominant systems: The first one is the system with both users designated dominant users, which is denoted by \mathcal{S}_0^* . The other two systems are the system with only one user designated dominant user. When the system designates user i a dominant user, it is denoted by \mathcal{S}_i^* for $i \in \{1, 2\}$.

In system \mathcal{S}_1^* , dominant user 1 can transmit a dummy packet if his queue is empty. Otherwise, he transmits a real packet. In system \mathcal{S} , the packet transmission of user 1 interferes with that of user 2 if and only if $Q_1(t) > 0$. However, user 1 in system \mathcal{S}_1^* always interferes with user

2 by transmitting either real packets if $Q_1(t) > 0$, or dummy packets if $Q_1(t) = 0$. It can be expected that $Q_2(t)$ in system S_1^* is larger than that in system S due to more frequent unsuccessful decoding caused by dummy packet transmissions from user 1. Additionally, $Q_1(t)$ in system S_1^* is also larger than that in system S since arriving packets to user 1 always find him busy with a dummy packet transmission when $Q_1(t) = 0$. For system S_2^* with user 2 being stochastic dominant user, the role of each user is interchanged. Accordingly, it is expected that $Q_1(t)$ and $Q_2(t)$ in system S_2^* are always larger than those in system S .

For system S_0^* , where both users are dominant users, it can be envisioned that $Q_1(t)$ and $Q_2(t)$ in system S_0^* are always larger than those in system S . Therefore, we can come to the conclusion that $Q_1(t)$ and $Q_2(t)$ in any stochastic dominant system would be at least larger than those in system S , if the queueing process starts with the same initial conditions in both systems. It thus follows that if a set of λ_1 and λ_2 makes both users' queue stable in a dominant system, this set makes the original system stable as well.

Let $\Lambda_{x,i}^*$, $i = 0, 1, 2$, denote the conditional stability region of dominant system S_i^* ; that is, a set of λ_1 and λ_2 guaranteeing stability of the dominant system given (re)transmission probabilities x_1 and x_2 . The entire conditional stability region of the dominant systems, denoted by $\Lambda_{\mathbf{x}}^*$, is expressed as

$$\Lambda_{\mathbf{x}}^* \equiv \bigcup_{i=0}^2 \Lambda_{x,i}^*. \quad (12)$$

Since the queue length of stochastic dominant systems is equal to, or larger than the original system with a given set of the mean packet arrival rates, the relation between the stability regions of two systems becomes

$$\Lambda_{\mathbf{x}} \supseteq \Lambda_{\mathbf{x}}^*. \quad (13)$$

In addition to (13), if we can show later $\Lambda_{\mathbf{x}} \subseteq \Lambda_{\mathbf{x}}^*$, it can be proved that $\Lambda_{\mathbf{x}} \equiv \Lambda_{\mathbf{x}}^*$.

III. ANALYSIS AND RESULTS

1) *System S_0^** : In the dominant system S_0^* , both users are dominant users. This means that no user's queue goes empty due to dummy packets. Based on Loynes' theorem [14], which shows that a queueing system is stable only if the mean packet arrival rate to user i 's queue is less than his service rate, we can see that user 1's queue is stable if

$$\lambda_1 < x_{1\{1,0\}} + x_{1\{1,2\}} \triangleq \mathcal{A}_{\mathbf{x}}, \quad (14)$$

where $x_{1\{1,0\}} = (p_1 + q_1)r_2$ denotes the transmission success probability of user 1, when he is the only transmitting user in a slot and user 2 doesn't. In addition, $x_{1\{1,2\}} = p_1q_2 + q_1p_2$ is the transmission success probability of user 1 when user 1 and 2 transmit at the same time in a slot.

Similarly, user 2's queue becomes stable if

$$\lambda_2 < x_{2\{0,2\}} + x_{2\{1,2\}} \triangleq \mathcal{B}_{\mathbf{x}}, \quad (15)$$

where $x_{2\{0,2\}} = (p_2 + q_2)r_1$ and $x_{2\{1,2\}} = p_2q_1 + q_2p_1$ denote the (re)transmission success probability of user 1 when only user 1 transmits in a slot and the (re)transmission success probability of user 2 when both users transmit in a slot, respectively. As a result, system S_0^* is stable under the following region:

$$\Lambda_{\mathbf{x},0}^* = \{(\lambda_1, \lambda_2) | \lambda_1 < \mathcal{A}_{\mathbf{x}}, \lambda_2 < \mathcal{B}_{\mathbf{x}}\}. \quad (16)$$

In Fig. 1, $\Lambda_{\mathbf{x},0}^*$ is shown as a rectangle defined by $\mathcal{A}_{\mathbf{x}}$ and $\mathcal{B}_{\mathbf{x}}$.

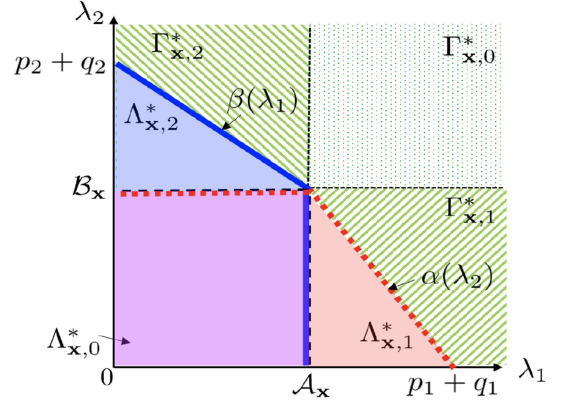


Fig. 1. Stability and instability regions.

2) *System S_2^** : In system S_2^* , user 2 is designated as a dominant user. In contrast to system S_0^* , since user 1 in system S_2^* has only real packets, his queue can be empty occasionally. To analyze user 1's queueing process, denote by π_k the (steady-state) probability that user 1's queue has k packets. Letting \hat{a}_k be the probability that k packets arrive at user 1 according to Poisson process with mean λ_1 , we can write π_k for $k \geq 0, 1, \dots$ as

$$\begin{aligned} \pi_k &= \hat{a}_k \pi_0 + \sum_{i=1}^k (\hat{a}_{k-(i-1)} \mu_1 + \hat{a}_{k-i} (1 - \mu_1)) \pi_i \\ &\quad + \hat{a}_0 \mu_1 \pi_{k+1}, \end{aligned} \quad (17)$$

where μ_1 denotes the probability that a packet of user 1's queue is successfully (re)transmitted. We get μ_1 as

$$\mu_1 = (p_1 + q_1)r_2 + p_1q_2 + q_1p_2 = \mathcal{A}_{\mathbf{x}}. \quad (18)$$

Let us define the probability generating functions (PGFs) of user's queue length and packet arrivals respectively as

$$\Pi(z) = \sum_{k=0}^{\infty} \pi_k z^k \quad \text{and} \quad A_1(z) = \sum_{k=0}^{\infty} \hat{a}_k z^k. \quad (19)$$

Using (17) and (19), the PGF of user 1's queue length is given by

$$\begin{aligned} \Pi(z) &= \frac{A_1(z)(z - \mu_1 + z(1 - \mu_1))}{z - A_1(z)(\mu_1 + z(1 - \mu_1))} \pi_0 \\ &= \frac{V_1(A_1(z))(z - 1)}{z - V_1(A_1(z))} \pi_0, \end{aligned} \quad (20)$$

where $V_1(z)$ is expressed as

$$V_1(z) = \mu_1 z \sum_{k=1}^{\infty} ((1 - \mu_1)z)^{k-1} = \frac{\mu_1 z}{1 - (1 - \mu_1)z}. \quad (21)$$

In (25), using $\lim_{z \rightarrow 1} \Pi(z) = 1$ we have $\pi_0 = 1 - \frac{\lambda_1}{\mu_1}$.

Let $\beta(\lambda_1)$ denote the service rate for user 2's queue. It is important to note that $\beta(\lambda_1)$ depends on the state of user 1's queue, i.e., empty or not. We can write it as

$$\begin{aligned} \beta(\lambda_1) &= (x_{2\{0,2\}} + x_{2\{1,2\}})(1 - \pi_0) + (p_2 + q_2)\pi_0 \\ &= (p_2(1 - p_1) + q_2(1 - q_1))(1 - \pi_0) + (p_2 + q_2)\pi_0. \end{aligned} \quad (22)$$

By applying Loynes' theorem to user 2, if the arrival rate of user 2 is less than $\beta(\lambda_1)$, i.e., $\lambda_2 < \beta(\lambda_1)$, we can see that user 2's queue is stable. In

addition, since user 1 is a dominant user, his queue is stable if $\lambda_1 < \mathcal{A}_x$. Accordingly, the conditional stability region of \mathcal{S}_2^* is expressed as

$$\Lambda_{x,2}^* = \{(\lambda_1, \lambda_2) | \lambda_1 < \mathcal{A}_x, \lambda_2 < \beta(\lambda_1)\}. \quad (23)$$

In Fig. 1, $\Lambda_{x,2}^*$ is depicted as a trapezoidal region whose circumference is depicted by a blue solid-line.

3) *System \mathcal{S}_1^** : Finally, let us investigate the stability region of dominant system \mathcal{S}_1^* , where user 1 is a dominant user. For the non-dominant user 2, let ϕ_k denote the (steady-state) probability that k packets are in user 2's queue, whereas \check{a}_k denotes the probability that k packets arrive at user 2 according to Poisson process with mean λ_2 . As in (17), ϕ_k becomes

$$\begin{aligned} \phi_k &= \check{a}_k \phi_0 + \sum_{i=1}^k (\check{a}_{k-(i-1)} \mu_2 + \check{a}_{k-i} (1 - \mu_2)) \phi_i \\ &\quad + \check{a}_0 \mu_2 \phi_{k+1}, \end{aligned} \quad (24)$$

where $\mu_2 = (p_2 + q_2)r_1 + p_2q_1 + q_2p_1 = \mathcal{B}_x$.

Furthermore, we define the PGF of the queue length of user 2 and the number of arriving packets to this user, respectively, as

$$\Phi(z) = \sum_{k=0}^{\infty} \phi_k z^k \quad \text{and} \quad A_2(z) = \sum_{k=0}^{\infty} \check{a}_k z^k. \quad (25)$$

We can find $\Phi(z)$ as

$$\begin{aligned} \Phi(z) &= \frac{A_2(z)(z - \mu_2 + z(1 - \mu_2))}{z - A_2(z)(\mu_2 + z(1 - \mu_2))} \phi_0 \\ &= \frac{V_2(A_2(z))(z - 1)}{z - V_2(A_2(z))} \phi_0, \end{aligned} \quad (26)$$

where $V_2(z)$ is expressed as

$$V_2(z) = \mu_2 z \sum_{k=1}^{\infty} ((1 - \mu_2)z)^{k-1} = \frac{\mu_2 z}{1 - (1 - \mu_2)z}. \quad (27)$$

From $\lim_{z \rightarrow 1} \Phi(z) = 1$ we get $\phi_0 = 1 - \frac{\lambda_2}{\mu_2}$.

Let $\alpha(\lambda_2)$ denote the service rate for user 1, which can be expressed as

$$\alpha(\lambda_2) = (x_{1\{1,0\}} + x_{1\{1,2\}})(1 - \phi_0) + (p_1 + q_1)\phi_0. \quad (28)$$

By Loynes' theorem to user 1, if the arrival rate of user 1 is less than $\alpha(\lambda_2)$, i.e., $\lambda_1 < \alpha(\lambda_2)$, we can see that user 2's queue is stable. In addition, since user 1 is a dominant user, his queue is stable if $\lambda_2 < \mathcal{B}_x$. Accordingly, the stability region of \mathcal{S}_1^* is expressed as

$$\Lambda_{x,1}^* = \{(\lambda_1, \lambda_2) | \lambda_1 < \alpha(\lambda_2), \lambda_2 < \mathcal{B}_x\}. \quad (29)$$

Fig. 1 illustrates $\Lambda_{x,1}^*$ whose circumference is depicted by a red dotline. Notice that $\Lambda_{x,0}^* \subset \Lambda_{x,1}^*$, $\Lambda_{x,0}^* \subset \Lambda_{x,2}^*$, and $\Lambda_{x,0}^* \subset (\Lambda_{x,1}^* \cup \Lambda_{x,2}^*)$. In addition, it can be seen that $\alpha(\lambda_2) \rightarrow p_1 + q_1$ as $\lambda_2 \rightarrow 0$, and $\beta(\lambda_1) \rightarrow p_2 + q_2$ as $\lambda_1 \rightarrow 0$.

Now we will show that the stability region of the stochastic dominant systems is equal to that of the original system by using the *instability* region of two systems. To begin with, let $\Gamma_{x,i}^*$ for $i \in \{0, 1, 2\}$ be the instability region of dominant system \mathcal{S}_i^* . It can be expected that the entire instability region of the dominant systems is the union of each instability region:

$$\bigcup_{i=0}^2 \Gamma_{x,i}^* = \bigcup_{i=0}^2 \Lambda_{x,i}^* = \bar{\Lambda}_x. \quad (30)$$

To find $\Gamma_{x,0}^*$, let us consider $\Lambda_{x,0}^* = \{(\lambda_1, \lambda_2) | \lambda_1 < \mathcal{A}_x, \lambda_2 < \mathcal{B}_x\}$. If arriving (real) packets start filling up each user's queue, dummy packet transmissions could gradually disappear. This implies that the queueing process of dominant system \mathcal{S}_0^* becomes *indistinguishable* from that of the original system \mathcal{S} . This takes place if $\lambda_1 \geq \mathcal{A}_x$ and $\lambda_2 \geq \mathcal{B}_x$. This makes both queues in system \mathcal{S}_0^* unstable, which also makes the original system \mathcal{S} unstable. Therefore, the instability region for system \mathcal{S}_0^* is expressed as

$$\Gamma_{x,0}^* = \{(\lambda_1, \lambda_2) | \lambda_1 \geq \mathcal{A}_x, \lambda_2 \geq \mathcal{B}_x\}, \quad (31)$$

which is shown in Fig. 1.

Secondly, let us find $\Gamma_{x,2}^*$. Note that non-dominant user 1's queue in system \mathcal{S}_2^* is stable if $\lambda_1 < \mathcal{A}_x$. For dominant user 2, his utilization is $\lambda_2/\beta(\lambda_1)$. As $\lambda_2/\beta(\lambda_1) \rightarrow 1$, we can see that dummy packet transmissions hardly occur such that dominant user 2's queue of system \mathcal{S}_2^* behaves asymptotically identical to that of system \mathcal{S} . Then, system \mathcal{S}_2^* is said to be *indistinguishable* from system \mathcal{S} . Since user 2's queue in system \mathcal{S}_2^* is unstable for $\lambda_2 \geq \beta(\lambda_1)$, the original system \mathcal{S} gets unstable as well. Thus, we get

$$\Gamma_{x,2}^* = \{(\lambda_1, \lambda_2) | \lambda_1 < \mathcal{A}_x, \lambda_2 \geq \beta(\lambda_1)\}. \quad (32)$$

By the same token, we can get $\Gamma_{x,1}^*$ as

$$\Gamma_{x,1}^* = \{(\lambda_1, \lambda_2) | \lambda_1 \geq \alpha(\lambda_2), \lambda_2 < \mathcal{B}_x\}. \quad (33)$$

In Fig. 1, $\Gamma_{x,1}^*$ and $\Gamma_{x,2}^*$ are illustrated. Since the original system gets also unstable for a set of λ_1 and λ_2 belonging to the instability region for its dominant system, we have

$$\bar{\Lambda}_x \supseteq \bar{\Lambda}_x^*. \quad (34)$$

Theorem 1: The stability region of hybrid uplink NOMA system is equal to that of its stochastic dominant system:

$$\Lambda_x \equiv \Lambda_x^*. \quad (35)$$

Proof: We can rewrite (34) as $\bar{\Lambda}_x \supseteq \bar{\Lambda}_x^* \Rightarrow \Lambda_x \subseteq \Lambda_x^*$. Using (13), i.e., $\Lambda_x \supseteq \Lambda_x^*$, we can complete the proof. ■

In Fig. 1, the circumference of Λ_x contains the blue-solid line for $0 \leq \lambda_1 \leq \mathcal{A}_x$ and the red dotline for $\mathcal{A}_x \leq \lambda_1 \leq \mathcal{A}_{\max}$.

Theorem 2: The boundary curve $f(\lambda_1)$, under which the stability region Λ_x lies, is characterized by

$$f(\lambda_1) = \begin{cases} \beta(\lambda_1), & \text{for } 0 \leq \lambda_1 \leq \mathcal{A}_x \\ \alpha^{-1}(\lambda_1), & \text{for } \mathcal{A}_x \leq \lambda_1 \leq \mathcal{A}_{\max}, \end{cases} \quad (36)$$

where we leave out the expression of $\alpha^{-1}(\lambda_1)$ for brevity.

Proof: Referring to $\Lambda_{x,1}^* \cup \Lambda_{x,2}^* \supset \Lambda_{x,0}^*$ in Fig. 1, we have

$$\Lambda_x \equiv \Lambda_{x,1}^* \cup \Lambda_{x,2}^*. \quad (37)$$

For $0 \leq \lambda_1 \leq \mathcal{A}_x$, user 2's queue is stable if $\lambda_2 < \beta(\lambda_1)$. Thus, $f(\lambda_1)$ follows $\beta(\lambda_1)$ in this range. On the other hand, the maximally allowable arrival rate at user 1's queue is found when $\lambda_2 = 0$, i.e., $\alpha(0) = \mathcal{A}_{\max}$. For $0 \leq \lambda_2 \leq \mathcal{B}_x$, the stability region lies in $\lambda_1 < \alpha(\lambda_2)$. It can be rewritten with respect to λ_1 , i.e., $\alpha^{-1}(\lambda_1) < \lambda_2$.

Proposition 1: The stability region Λ_x is convex if

$$\mathcal{A}_x/\mathcal{A}_{\max} + \mathcal{B}_x/\mathcal{B}_{\max} \geq 1, \quad (38)$$

where $\mathcal{A}_{\max} = p_1 + q_1$ and $\mathcal{B}_{\max} = p_2 + q_2$.

Proof: As shown in Fig. 2, we can draw a straight line $-\frac{\mathcal{B}_{\max}}{\mathcal{A}_{\max}}\lambda_1 + \mathcal{B}_{\max} = \lambda_2$. If $\lambda_2 \geq \mathcal{B}_x$ for $\lambda_1 = \mathcal{A}_x$, the stability region becomes convex. ■

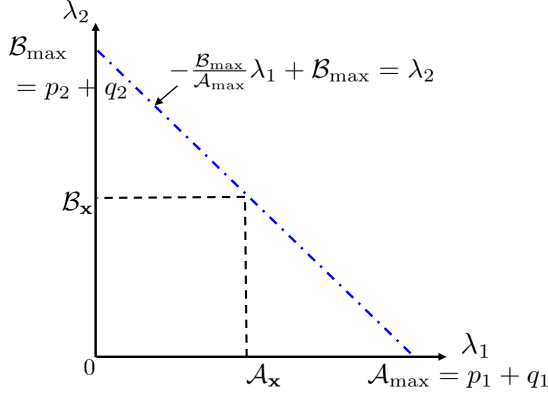


Fig. 2. Convexity of stability region.

Let us apply the mixed-strategy NE to the stability region. For the symmetric game, i.e., $p_1 = p_2 = p$, $q_1 = q_2 = q$, and $r_1 = r_2 = r$, let us see whether or not μ_i for $i \in \{1, 2\}$ can be nonnegative for the mixed-strategy NE in (6): We can write (18) as $\mu_1 = (p + q)r + 2pq = (2 - \frac{C_1 + C_2}{R})(1 - \frac{C_1 + C_2}{R}) - 2(1 - \frac{C_1}{R})(1 - \frac{C_1}{R}) = (C_1 + C_2)R + C_1^2 + C_2^2$, where we have used (6). Using $C_1 = C_2 + \epsilon$ for $\epsilon > 0$ and plugging it into μ_1 , we can rewrite $\mu_1 > 0$ in terms of R , C_1 , and C_2 as

$$R > \frac{C_1^2 + C_2^2}{C_1 + C_2} = C_2 + 0.5\epsilon + \frac{0.5\epsilon^2}{2C_2 + \epsilon}. \quad (39)$$

If $C_2 \gg \epsilon$ and $\epsilon < 1$, the above can be approximated as $R > C_2 + \epsilon \approx C_1$. This shows that if $R > C_1$, $C_1 = C_2 + \epsilon$ and $C_2 \gg \epsilon > 0$, we have $\mu_1 > 0$.

Proposition 2: In the symmetric game, the stability region becomes convex at the mixed-strategy NE if we have

$$C_2 + \epsilon \leq R \leq 1.5C_2 + 0.75\epsilon + \sqrt{\zeta}, \quad (40)$$

where $\zeta = 4.5C_1C_2 - 1.75(C_1^2 + C_2^2)$ and $C_2 > (\sqrt{2} - 0.5)\epsilon \approx 0.914\epsilon$.

Proof: In the symmetric game, recall that we should have $C_1 < R < C_1 + C_2$. Using $C_1 = C_2 + \epsilon$, we have $C_2 + \epsilon < R < 2C_2 + \epsilon$. This shows the strict inequality of the LHS in (40). In the symmetric game, the convexity condition of stability region in (38) becomes

$$r + 2pq/(p + q) \geq 0.5. \quad (41)$$

With (6) and (41), we write (41) in terms of R , C_1 , and C_2 as $R^2 - 1.5(C_1 + C_2)R + C_1^2 + C_2^2 \leq 0$. From this, if we have

$$\frac{1.5(C_1 + C_2) - \sqrt{\zeta}}{2} \leq R \leq \frac{1.5(C_1 + C_2) + \sqrt{\zeta}}{2}, \quad (42)$$

then the stability region is convex. Since the LHS of (42) is less than C_1 , we can write (42) as (40). Since the radicand ζ must be nonnegative, plugging $C_1 = C_2 + \epsilon$ into ζ , we have $\zeta = C_2^2 + \epsilon C_2 - 1.75\epsilon^2 \geq 0$. This holds if $C_2 \geq (\sqrt{2} - 0.5)\epsilon$. This is a necessary condition for ζ to be nonnegative. ■

It is notable that the stability region is always convex at the mixed-strategy NE in (6), if the RHS of (42) is larger than $C_1 + C_2$; that is, $C_1 + C_2 = 2C_2 + \epsilon < 1.5C_2 + 0.75\epsilon + \sqrt{\zeta}$. We then have $(0.5C_2 + 0.25\epsilon)^2 < \zeta \Rightarrow 3C_2^2 + 3\epsilon C_2 - \frac{29}{4}\epsilon^2 > 0$. If $C_2 \geq 1.13299\epsilon$, then the stability region is convex at the mixed-strategy NE.

Let us discuss numerical results with $\bar{\gamma} = 1$ in (7) and (8): Fig. 3 depicts the stability regions with various rewards and costs. Note

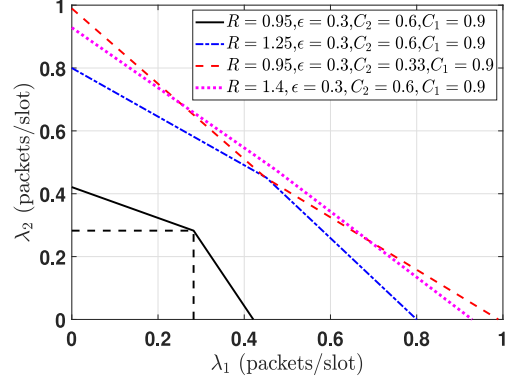
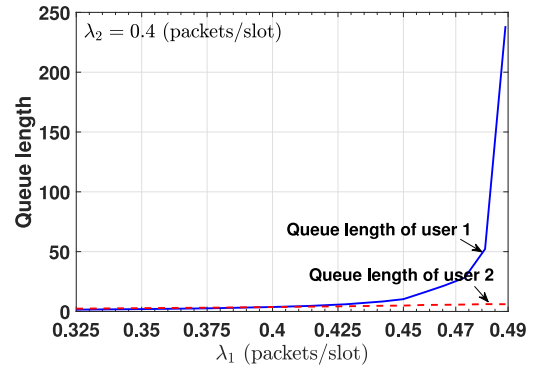

 Fig. 3. Stability regions (The small rectangle indicates the stability region of system \mathcal{S}_0^* for $R = 0.95$, $C_1 = 0.9$ and $C_2 = 0.6$.)


Fig. 4. Queue length vs. mean arrival rates.

that when R , C_1 and C_2 are given, we can determine p^* , q^* , and r^* with (6) and find $c_1 = (R(1 - p_i^*)p_i^*\bar{\gamma})/(P_1 E_1(\ln \frac{1}{p_i^*}))$ with P_1 and similarly c_2 .

First, let us examine the convexity of the stability region for the parameters given. If $C_2 = 0.6$, $\epsilon = 0.3$, and $C_1 = C_2 + \epsilon$, we have $1.5C_2 + 0.75\epsilon + \sqrt{\zeta} = 1.7435$. Thus, (40) holds for $R = 0.95$ and 1.25 , which guarantees the convexity of the stability region. The stability region is also convex for $R = 1.4$. It is observed that as R increases, which encourages the users to transmit, the stability region expands. For $R = 1.4$ (high reward), the stability region gets close to that of the ideal TDMA (or genie-aided), in which an omniscient centralized scheduler schedules a slot to two users perfectly depending on the state of two users' queue. Note that its stability region is $\lambda_1 + \lambda_2 \leq 1$. When C_1 and C_2 are respectively reduced to 0.63 and 0.33 from 0.9 and 0.6 , the users are more incentivized to transmit. In this case, the stability region is non-convex since (40) does not hold. However, the stability region seems close to that of the ideal TDMA system as well. We can come to the conclusion that while hybrid uplink NOMA is a distributed scheduler based on random access, it achieves the stability region close to the ideal TDMA system if either a high reward R and/or low cost C_i 's is considered.

In Fig. 4, the stability region with $R = 1.25$, $C_1 = 0.9$ and $C_2 = 0.6$ is verified. As shown, at $\lambda_2 = 0.4$, the maximum rate for user 1 cannot exceed $\lambda_1 = 0.49$, which is the boundary of the stability region. As λ_1 gets close to 0.49 in Fig. 4, the user 1's queue increases explosively.

Let us compare the hybrid uplink NOMA with OMA in terms of throughput. Let ϱ_N and ϱ_O denote the throughput of hybrid uplink NOMA and OMA system, respectively. In the symmetric game, ϱ_N

can be expressed as

$$\varrho_N = (1-r) (\Pr[Q_1 > 0, Q_2 = 0] + \Pr[Q_1 = 0, Q_2 > 0]) + 2(2pq + (p+q)r) \Pr[Q_1 > 0, Q_2 > 0]. \quad (43)$$

For OMA system, where a user exclusively uses one RRB, let Q and λ denote the queue length of a user who use one RRB and the mean rate of packet arrivals to the user. Then, ϱ_O is expressed as $\varrho_O = (1-r) \Pr[Q > 0]$. In order for hybrid uplink NOMA to benefit from statistical multiplexing by random access compared to OMA system, under the same traffic load $\lambda_1 + \lambda_2 = \lambda$, it is expected that

$$\varrho_N > \varrho_O \quad \text{or} \quad \varrho_N - \varrho_O > 0. \quad (44)$$

To see that (44) always holds, the joint probabilities $\Pr[Q_1 > 0, Q_2 = 0]$, $\Pr[Q_1 = 0, Q_2 > 0]$, and $\Pr[Q_1 > 0, Q_2 > 0]$ should be obtained. Since it is difficult to get these probabilities, *first* let us assume two cases, i.e., either $\Pr[Q_1 > 0, Q_2 = 0] = \Pr[Q > 0]$, or $\Pr[Q_1 = 0, Q_2 > 0] = \Pr[Q > 0]$. Then, it can be seen that $\Pr[Q_1 > 0, Q_2 = 0]$ (or $\Pr[Q_1 = 0, Q_2 > 0]$) and $\Pr[Q > 0]$ are cancelled out on the LHS and RHS in (44) so that (44) holds for two cases. *Second*, let us assume $\Pr[Q_1 > 0, Q_2 = 0] + \Pr[Q_1 = 0, Q_2 > 0] \geq \Pr[Q > 0]$. We then have $\varrho_N - \varrho_O = 2(2pq + (p+q)r) \Pr[Q_1 > 0, Q_2 > 0] > 0 > (1-r) (\Pr[Q > 0] - \Pr[Q_1 > 0, Q_2 = 0] + \Pr[Q_1 = 0, Q_2 > 0])$ so that (44) holds as well. *Finally*, let us consider $\Pr[Q_1 > 0, Q_2 = 0] + \Pr[Q_1 = 0, Q_2 > 0] < \Pr[Q > 0]$. We write (44) as $\varrho_N - \varrho_O = 2(2pq + (p+q)r) \Pr[Q_1 > 0, Q_2 > 0] > (1-r) (\Pr[Q > 0] - (\Pr[Q_1 > 0, Q_2 = 0] + \Pr[Q_1 = 0, Q_2 > 0])) > 0$. For $\lambda_1 + \lambda_2 = \lambda$, it is highly likely to see $\Pr[Q > 0] \leq \Pr[Q_1 > 0, Q_2 > 0] + \Pr[Q_1 > 0, Q_2 = 0] + \Pr[Q_1 = 0, Q_2 > 0]$. When it would hold, (44) holds too.

IV. CONCLUSION

This paper has examined hybrid uplink NOMA systems, where two users share one RRB based on NOMA random access such that 2 M users can be accommodated with M orthogonal RRBs. By incorporating (non-cooperative) game, we investigated the stability region of two-user hybrid uplink NOMA system. At the mixed-strategy NE, where two users are statistically multiplexed with competition, we

showed the convexity of the stability region depending on the rewards and costs. It has been demonstrated that the stability region of hybrid uplink NOMA system can be almost identical to that of the ideal TDMA system under some conditions.

REFERENCES

- [1] Y. Zhou, V. W. S. Wong, and R. Schober, "Stable throughput regions of opportunistic NOMA and cooperative NOMA with full-duplex relaying," *IEEE Trans. Wireless Commun.*, vol. 17, no. 8, pp. 5059–5075, Aug. 2018.
- [2] R. Xie, H. Yin, X. Chen, and Z. Wang, "Many access for small packets based on precoding and sparsity-aware recovery," *IEEE Trans. Commun.*, vol. 64, no. 11, pp. 4680–4694, Nov. 2016.
- [3] R. Hoshyari, F. P. Wathan, and R. Tafazolli, "Novel low-density signature for synchronous CDMA systems over AWGN channel," *IEEE Trans. Signal Process.*, vol. 56, No 4, pp. 1616–1626, Apr. 2008.
- [4] N. Zhang, J. Wang, G. Kang, and Y. Liu, "Uplink nonorthogonal multiple access in 5G systems," *IEEE Commun. Lett.*, vol. 20, no. 3, pp. 458–461, Mar. 2016.
- [5] Y. Gao, B. Xia, K. Xiao, Z. Chen, X. Li, and S. Zhang, "Theoretical analysis of the dynamic decode ordering SIC receiver for uplink NOMA systems," *IEEE Commun. Lett.*, vol. 21, no. 10, pp. 2246–2249, Oct. 2017.
- [6] H. S. Jang, H. Lee, and T. Q. S. Quek, "Deep learning-based power control for non-orthogonal random access," *IEEE Commun. Lett.*, vol. 23, no. 11, pp. 2004–2007, Nov. 2019.
- [7] Y. Liang, X. Li, J. Zhang, and Z. Ding, "Non-orthogonal random access for 5G networks," *IEEE Trans. Wireless Commun.*, vol. 16, no. 7, pp. 4817–4831, Jul. 2017.
- [8] Y. Wang, T. Wang, Z. Yang, D. Wang, and J. Cheng, "Throughput-oriented non-orthogonal random access scheme for massive MTC networks," *IEEE Trans. Commun.*, vol. 68, no. 3, pp. 1777–1793, Mar. 2020.
- [9] L. Liu, M. Sheng, J. Liu, Y. Dai, and J. Li, "Stable throughput region and average delay analysis of uplink NOMA systems with unsaturated traffic," *IEEE Trans. Commun.*, vol. 67, no. 12, pp. 8475–8488, Dec. 2019.
- [10] S. Han *et al.*, "Energy-efficient short packet communications for uplink NOMA-based massive MTC networks," *IEEE Trans. Veh. Technol.*, vol. 68, no. 12, pp. 12066–12078, Dec. 2019.
- [11] J. Choi, "NOMA-based random access with multichannel aloha," *IEEE J. Sel. Areas Commun.*, vol. 35, no. 12, pp. 2736–2743, Dec. 2017.
- [12] J.-B. Seo, B. C. Jung, and H. Jin, "Performance analysis of NOMA random access," *IEEE Commun. Lett.*, vol. 22, no. 11, pp. 2242–2245, Aug. 2018.
- [13] J. Choi and J.-B. Seo, "Evolutionary game for hybrid uplink NOMA with truncated channel inversion power control," *IEEE Trans. Commun.*, vol. 67, no. 12, pp. 8655–8664, Dec. 2019.
- [14] R. M. Loynes, "The stability of a queue with non-independent interarrival and service times," *Proc. Cambridge Philos. Soc.*, vol. 58, no. 3, pp. 494–520, Jul. 1962.